ACCURACY OF THE DETERMINATION OF THE CURRENT DENSITY VIA FOUR SATELLITES

Patrick Robert, Alain Roux, Gérard Chanteur

Centre d'étude des Environnements Terrestre et Planétaires, CNRS-UVSQ, Vélizy, France

Malcolm Dunlop

The Blackett Laboratory, Imperial College, London, UK

ABSTRACT

The determination of the current density from the magnetic field measurements on board the 4 Cluster spacecraft is a key issue to the success of the mission. Earlier studies have been concentrated on the identification of a single geometric parameter characterizing the shape of the tetrahedron and its influence upon the accuracy of the determination of the current density. We suggest to use two parameters F (for flattening) and L (for lengthening). The accuracy of the estimate of **J** as a function of these two parameters is studied via numerical simulation based on a large number of geometrical configurations for the tetrahedron. The possible relationship between div(**B**) and the uncertainty in the determination of the current density is studied, as well as the possible influence of the direction of the current with respect to the largest of the faces of the tetrahedron.

1. INTRODUCTION

The Cluster mission will enable simultaneous measurements of the vector magnetic field at the 4 vertices of a tetrahedron [1]. The shape of this tetrahedron evolves along the mean trajectory of the 4 spacecraft. Thanks to a contour integral method (CI) or to a barycentrique coordinate method (BC), it is possible to estimate the current density **J** and the divergence of **B** inside the tetrahedron [2, 3]. These estimates are subject to various sources of errors [4, 5, 6]. There are basically two types of errors. The first one is related to the uncertainties in the measurement of **B**, and to the uncertainties in the localization and the attitude of the 4 spacecraft. The second one is related to the linear interpolation which is made between the various measurement points. The influence of these errors on the accuracy of the estimate of **J** or div(**B**) are also related to the shape of the tetrahedron [4, 5, 6]. We discuss here the following questions: (i) how to characterize easily the shape of a given tetrahedron, (ii) what is the relation between the geometrical shape of the tetrahedron and the accuracy of the determination of **J** via the estimate of curl(**B**) , (iii) can div(**B**) be used as an estimate of the error ΔJ, and (iv) when the tetrahedron is relatively flat, is there a relation between the accuracy of the determination of **J** and the orientation of the current with respect to the orientation of the tetrahedron? These questions are studied, with the help of a numerical simulation based on a large number of possible tetrahedron and a model for the current structure.

2. THE SHAPE OF THE TETRAHEDRON

2.1. The 1D geometric criterion

Several geometric parameters were proposed [4,6,7,8] to characterize the shape of a tetrahedron, with only one parameter. The concept of "fractional dimension" [7] has been introduced to characterize the transition on a linear, a flat, and a regular tetrahedron. Several other 1-D parameters have been studied [4] to characterize the shape of the tetrahedron and to try to relate this shape to the accuracy of the measurement of the current density computed from the magnetic field measurements. Nevertheless, it seems that even the "best" 1-D parameter is not sufficient to characterize the shape of the tetrahedron and therefore do not provide an accurate index for the a priori assessment of the accuracy of the determination of **J** [4]. In the present work we suggest to use a set of two parameters to characterize the shape and we test the efficiency of the relation between these parameters and the accuracy of the determination of **J**.

2.2. The Cluster inertial ellipsoid

To describe the shape of a given irregular tetrahedron we use the concept of an inertial ellipsoid [8], which is that which fits best the tetrahedron. This ellipsoid is derived from the inertial tensor defined as:

$$T = \begin{bmatrix} Txx & Txy & Txz \\ Tyx & Tyy & Tyz \\ Tzx & Tzy & Tzz \end{bmatrix} \qquad \text{with} \qquad Txy = \sum (xi - xg)(yi - yg)$$

The eigen vectors determine the directions and the lengths of the semi-major, the semi-middle and the semi-minor axis of the ellipsoid. This is a very simple way to approach the shape of a tetrahedron, since we can have directly a quick look at the global shape: for instance an ellipsoid reduced to a sphere corresponds to a regular tetrahedron, with an inter-spacecraft distance equal to the radius, an ellipsoid reduced to a plane corresponds to a flat tetrahedron, and an ellipsoid reduced to a line corresponds, of course, to the alignment of the 4 spacecraft.

2.3. The Flattening and Lengthening parameters

The inertial ellipsoid gives directly an information about the shape of a tetrahedron with 3 parameters *a, b, c* corresponding to the length of the 3 axes. We can easily reduce this number to only 2 parameters, by defining a "Lengthening parameter " and a "Flattening parameter " derived from the 3 axes as:

$$\mathrm{L} = 1 - \frac{b}{a} \qquad\qquad \mathrm{F} = 1 - \frac{c}{b}$$

Of course a regular tetrahedron has a Lengthening (L) and a Flattening (F) equal to zero ($a=b=c$), a long tetrahedron has a Lengthening close to 1 ($a>>b$), a plane tetrahedron has a Flattening close to 1 ($b>>c$), and a both long and plane tetrahedron has Lengthening and Flattening both close to 1 ($a>>b>>c$). Thus, only 2 parameters contains all the necessary information characterizing the shape of the ellipsoid, since of course *b* and *c* axis can be rebuild from *a* (giving the absolute size) and from L and F via $b=a(1\text{-L})$ and $c=a(1\text{-L})(1\text{-F})$.

2.4. Types of tetrahedra

The L and F parameters allows us to define 5 types of tetrahedra. Figure 1 shows where, in the L-F plane, are each type of tetrahedron. For low values of L and F we can define a "Balls shaped tetrahedra" (bottom left corner of the L-F diagram) corresponding to the pseudo-regular tetrahedra. For a high value of F and a low value of L (top left corner of the L-F diagram) the ellipsoid is nearly a flat circle and we can define it as "Dishes shaped". At the opposite side (bottom right corner) we can find a long ellipsoid with a pseudo circular section, that we can define as a "Cigars shaped". At least, at the top right corner, we can find tetrahedra which are both flat and elongated, and we can call this type the "Knife Blade shaped". Tetrahedra that do not belong to one of these categories or types, because they do not have a specific shape, will be referred to "Potatoes type" and are located at the center of the L-F diagram.

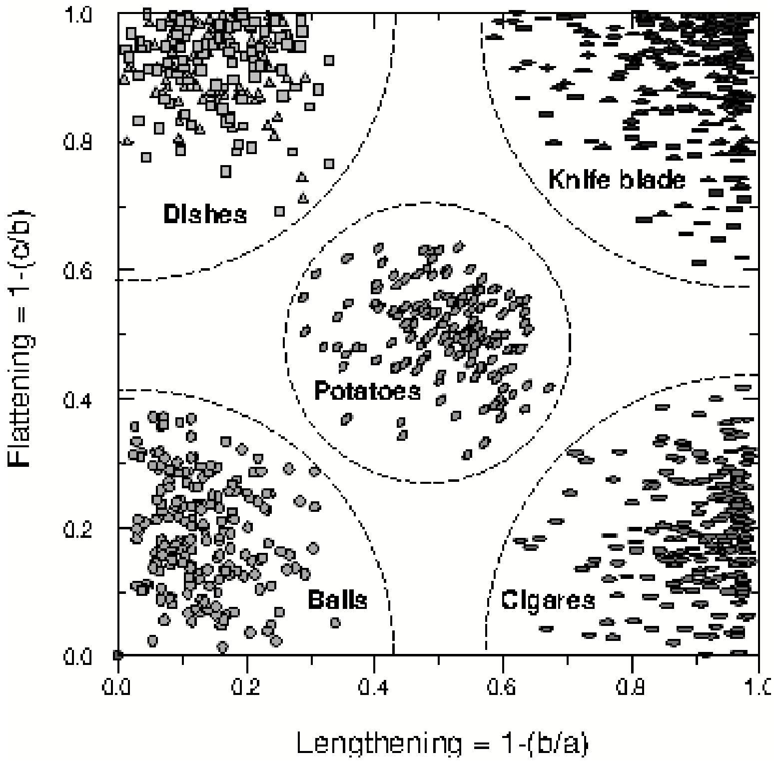

Figure 1: The five types of tetrahedra: Balls, Dishes, Cigares, Knife Blade, and Potatoes.

2.5. <u>The characteristic of the Cluster tetrahedron along the orbit</u>

The configuration of the Cluster tetrahedron is not frozen along the orbit, it varies with time. In particular, it is possible to have a regular tetrahedron in two points of an given orbit [5,8], but in the between the shape of the tetrahedron can take any other configuration. On figure 2, the shape of the Cluster tetrahedron is computed and plotted in a L-F diagram along a whole orbit. The orbit has been given by ESA [9], and established on the basis of a launch in November 1995. Although the launch is delayed, the arguments remain the same. The time step is 6 minutes, and the arrow indicates the direction of the motion. The apogee corresponds to the portion of the figure where the different points are very close together, the velocity being low and the shape slowly varying. The perigee corresponds to the portion of the figure where the points are widely spaced, because the spacecraft velocity along the average trajectory is large.

On figure 2-a (1995, December 24), in accordance with the request that the tetrahedron should be regular at 2 points along the orbit, the first point is located near (L,F) = (0.28, 0.01) , and the tetrahedron is regular only during a very short period. The second point where the tetrahedron is regular corresponds to a longer period, from (L,F) = (0.21, 0.01) to (L,F) = (0.01, 0.16). These two periods where the tetrahedron is regular are of course located in the region of the "Balls type". During the rest of the time, the L-F parameters take any value, in particular the tetrahedron is absolutely flat (F=0.99) for 2 points along the orbit, but never completely linear (the maximum value of L is 0.8 near the perigee). For another example shown on figure 2-b (1996, June 24) the conclusions remain the same. During the course of the Cluster mission, all possible shape of tetrahedra are expected, and thus, simulations must take into account any possible value in the L-F plane.

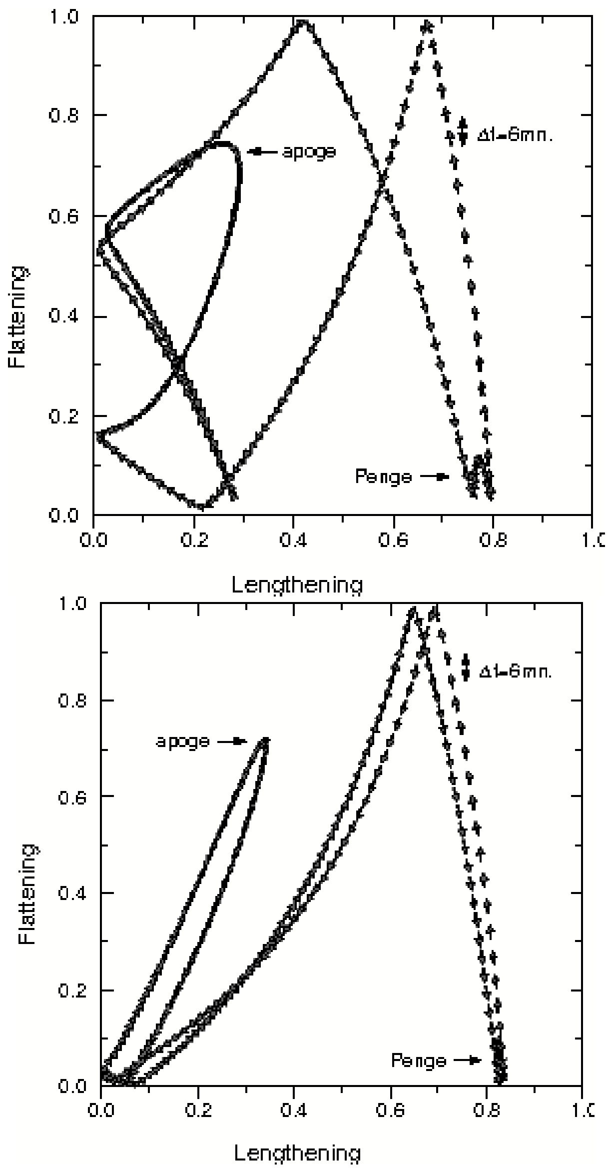

Figure 2: Evolution of the shape of the Cluster tetrahedron along its trajectory in a L-F diagram (data provided by ESA). a: December 24, 1995 (top); b: June 24, 1996 (bottom)

3. THE SIMULATION METHOD

3.1. <u>The tetrahedra reservoir</u>

The shape of the tetrahedron being characterized by the L-F parameter, we will try to identify a relationship between the value of these parameters and the accuracy of the measurement of the estimate of curl(**B**) and div(**B**). First, to be sure that any shape are taken into account, we have built a "tetrahedra reservoir" of about 1000 tetrahedra. This reservoir should represent a wide variety of configurations and therefore be homogeneous in the L-F plane. Figure 3 shows that there is indeed an homogeneous distribution of representative points. To avoid a bias, all the tetrahedra have the same mean inter-spacecraft distance <D> = (d1+d2+...+d6)/6, arbitrary fixed at 1000 km.

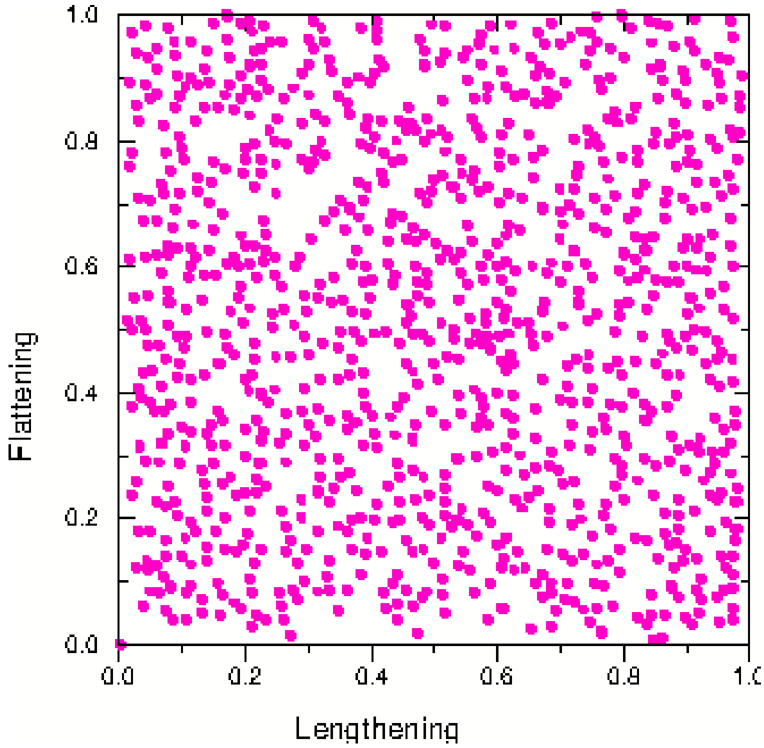

Figure 3: The tetrahedra reservoir used in the paper. Notice the homogeneous coverage of the L-F plane

3.2. The current structure models

The goal is to simulate the crossing of a current structure by the Cluster constellation. We have therefore to define a current structure model. The chosen model is described in figure 4: it consists of a cylindrical current tube, with an homogeneous current density (figure 4-a), or a gaussian current density profile (figure 4-b). In all cases, we assume that the size of the Cluster tetrahedron is smaller than the size of the current density structure, so all the spacecraft are simultaneously located inside the current density structure. Typical values are <D>=1000 km, R or σ=5000 km, Jo=10^{-8} A.m^{-2}.

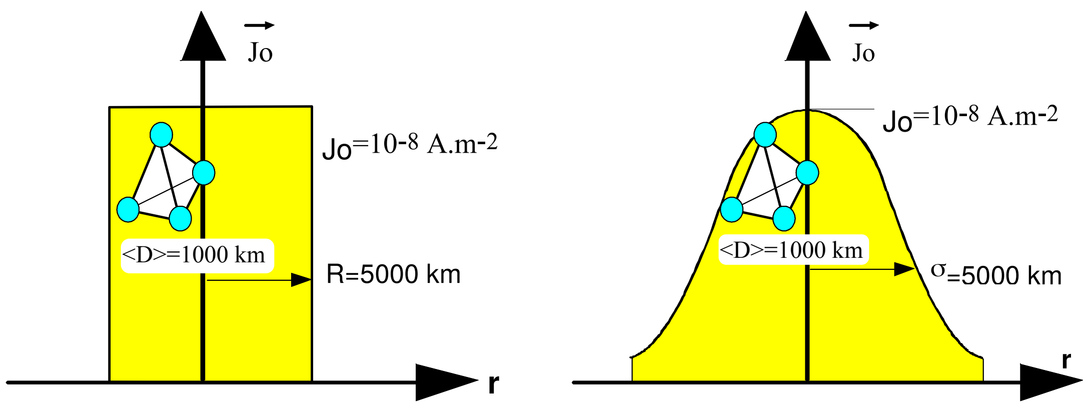

Figure 4: Current structure models (a) current tube with homogeneous current density profile (left); (b) same with gaussian current density profile (right).

3.3. The computation of J and div(**B**)

When the Cluster tetrahedron is inside the current density structure, we compute curl(**B**) and div(**B**) from the barycentric coordinate method. The uncertainty on the measurements is simulated by adding of a random noise on the 3 components of the 4 $\mathbf{B}_i$ vectors. Similarly a random noise is added to the 4 $\mathbf{S}_i$ vectors describing the positions of the 4 spacecraft. The amplitude ΔB of the noise added on the 3 magnetic field vectors is independent of the components, and proportional to the modulus of **B**. The uncertainty ΔS in the knowledge of the spacecraft position is taken to be proportional to <D>, the average interspacecraft distance. ΔB/B or ΔS/S represent the relative accuracy in the determination of $\mathbf{B}_i$ and $\mathbf{S}_i$. Typical values for ΔS/S is 1%, which corresponds to the nominal value given by the Cluster project. By computing **J**=curl(**B**)/μo from the perturbed simulated data, we obtain an estimate of the **J** vector which is compared to the real value given by the model. Thus the accuracy of the estimate of J, ΔJ/J, can be estimated. Previous works [2,4] have shown that the errors ΔB/B or ΔS/S have the same effect on the accuracy ΔJ/J. Therefore we will, for the sake of simplicity, only consider the perturbation ΔS/S. This computation is made for all the tetrahedra taken from the previously defined reservoir, thus all the L-F plane is covered.

4. RESULTS

4.1. Influence of the shape of the tetrahedron on the error ΔJ/J

First we consider an homogeneous current density profile, and therefore there is no error associated with the linear interpolation between the measurement made at the 4 s/c locations; only the uncertainties on the positions measurement are taken into account (<ΔS/S>=1%, ΔB/B=0). The main results are shown in figure 5, where we have plotted the relative accuracy ΔJ/J in a L-F diagram. The size and the colors of the circles indicate the values of ΔJ/J: for ΔJ/J=0, the radius of the circle is null, the largest circles correspond to ΔJ/J ≥100%.

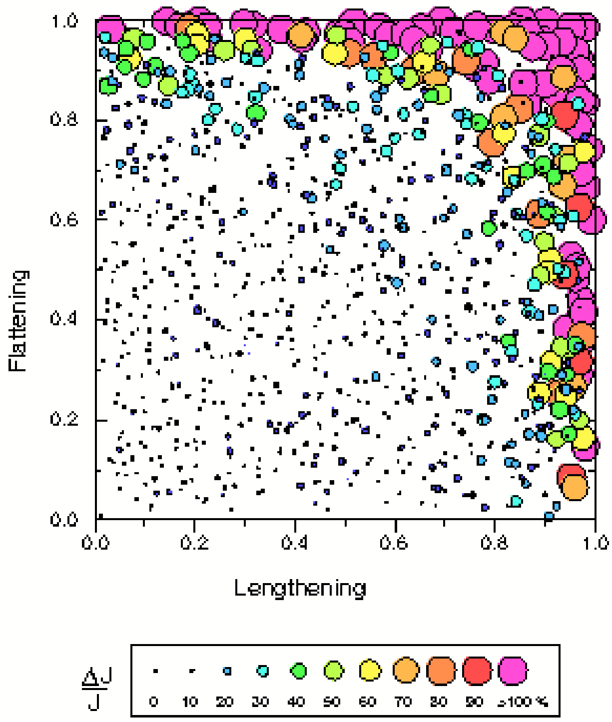

Figure 5: Influence of the shape of the tetrahedron on the estimate of ***J.***

The main conclusion is that for a large fraction of the diagram, corresponding to the "Balls type" and to a large part of the "Potatoes type", the accuracy ΔJ/J remains below a reasonable value (less than 20%). But for values of the Lengthening or Flattening parameter larger than about 0.6, the errors reach 30% or more.
For L or F > 0.9, which corresponds to a very long or a very flat tetrahedron, the error can reach 100% and more, especially of course when both F and L gets of the order of unity. As a matter of fact, the error increase roughly with the radius $r=(L^2+F^2)^{1/2}$, but this variation is not linear.

4.2. Influence of the shape of the tetrahedron on the estimate of div(**B**)/curl(**B**)

The results are shown in the figure 6. The values of div(**B**) and curl(**B**) are the estimated values, simulating the measurement values. Notice that the tetrahedron reservoir being homogeneous, the theoretical value of curl(**B**) is the same for all the points, and the curl(**B**) estimated values differs from the theoretical ones according the results of figure 5. The theoretical value of div(**B**) is obviously equal to zero. Since div(**B**) is not a normalized quantity, we have choose to display the estimate of the ratio div(**B**)/curl(**B**) ratio rather than the absolute value of div(**B**). The color code is the same as for ΔJ/J. Roughly speaking, the diagram looks the same, the "Balls" and "Potatoes" types gives the lower values of the divergence, and a large value of L or F leads to a large value of the estimated divergence.

4.3. Relationship between the error ΔJ/J and div(**B**)/curl(**B**)

Since the div(**B**)/curl(**B**) diagram looks the same as the ΔJ/J diagram, one could consider the estimate ratio div(**B**)/curl(**B**) as an estimate of the error ΔJ/J. This is statistically true (see previous subsection), but a more careful investigation shows that there is no one to one correspondence between the two diagrams; a large value of ΔJ/J can correspond to a small value of div(**B**)/curl(**B**) ratio, and vice-versa, good estimates of J can correspond to large value of the divergence (large div(**B**)/curl(**B**)). This is particularly true for large values of L or F.

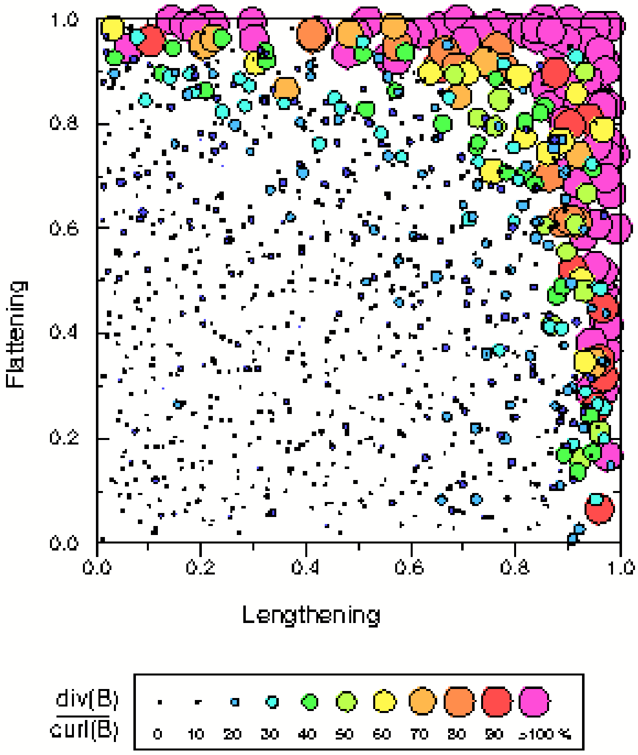

*Figure 6: Influence of the shape of the tetrahedron on the estimate of div(**B**)/curl(**B**).*

In order to characterize the possible relationship between ΔJ/J and div(**B**)/curl(**B**), we have plotted it in the same figure (figure 7). The color code and the symbols corresponds to the family of the tetrahedra. A possible relationship between theses two parameter would result in the alignment of the representative points. This is not observed; the distribution of the points has no preferred direction. Of course the area of the "Balls" (round symbols) is restricted to the central part of the diagram, close to zero, while the other types cover all the diagram. The non-existence of a correlation between div(**B**) and ΔJ can be explained by the fact that their computation does not use the same components in the tensor ∇**B**: the divergence is obtained from the diagonal terms, while the curl is built from the non-diagonal terms. Theses terms being perturbed by the addition of a independent random noise on the 12 components defining the 4 spacecraft positions to simulate the uncertainties on the measurement of theses position, the corresponding errors on the gradient tensor are not dependant. Practically, if the errors on the various components are effectively independent, this means that we cannot use the value of the divergence to estimate the error ΔJ.

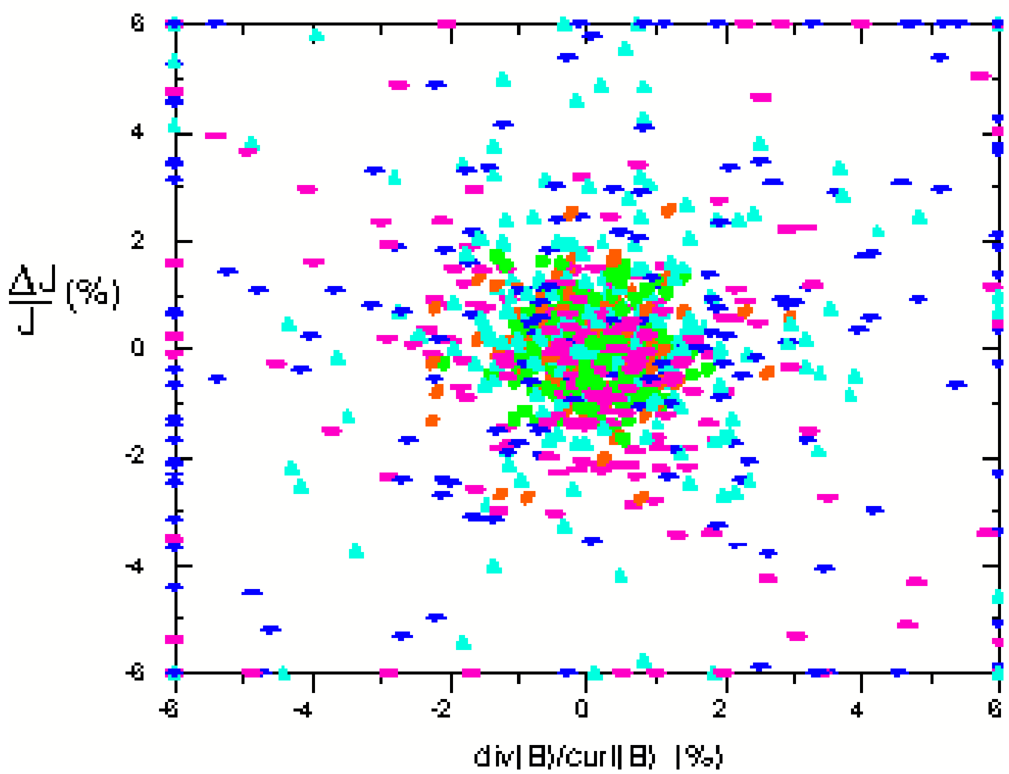

*Figure 7: Relationship between the error ΔJ/J and the ratio div(**B**)/curl(**B**).*

4.4. <u>Influence of the direction of the current on the error ΔJ/J</u>

In the present subsection we investigate the potential influence of the direction of the current with respect to the largest face of the tetrahedron. Figure 8 show the result: the relative error ΔJ/J is plotted versus the angle θ which is the angle between the direction of the current and the normal to the main plane of the tetrahedron. The main plane of the tetrahedron is defined as the plane containing the semi-major and semi-meddle axis of the inertial ellipsoid, thus the normal to this plane is the semi-minor axis.

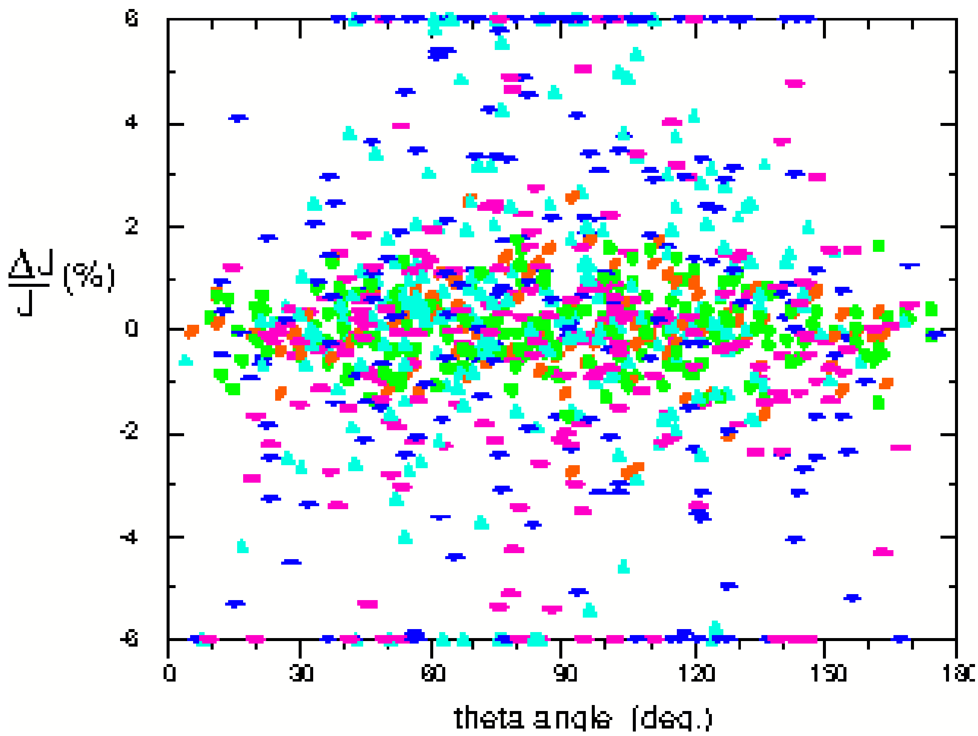

Figure 8: Influence of the current density direction on the error ΔJ/J.

A color code and a symbol are used to separate the different families of tetrahedra. The "Balls" are useless because the main plane has no meaning for a sphere. On could expect to find in this diagram a relationship between ΔJ/J and θ, showing for instance that the quality of the estimate would be better when the current is orthogonal to the main plane. In fact the (expected) minimum of ΔJ/J for θ=0 or θ=180° is not clear. One can observe a slight tendency for the "Dishes", for which the main plane has of course the clearest meaning, but this relationship is not very obvious. Practically, except for values of θ very close to 0 ° or 180° , it seems that the angle θ does not organize the diagram and therefore error ΔJ/J is not related to this angle.

14.5 Heterogeneous current profile

The estimate of the current density inside the volume defined by the tetrahedron relies on the assumption that the magnetic field varies linearly between two spacecraft. If the current density profile is not homogeneous in space (as it will be the case), the higher orders derivatives introduce a supplementary source of errors. To study this effect, we use a gaussian shape for the current density profile, such as the one shown in figure 4-b, and define a heterogeneity factor h=<D>/σ where <D> is the mean inter-spacecraft distance and σ is the root mean square deviation of the Gaussian. In order to better illustrate the effect of heterogeneity of the profile, we neglect, hereafter, the uncertainties ΔB/B and ΔS/S which are set to zero.

Figure 9 shows the relationship between the shape of the tetrahedron, again defined by the L and F parameters, and the accuracy ΔJ/J of the estimate, for a low value of the heterogeneity factor. The chosen value h=0.1 being low, the profile of the current structure is not very heterogeneous at the scale of the Cluster tetrahedron, so the relative error ΔJ/J is very low, except for large values of L or F. For large values of L and F we find a result similar to the homogeneous case with a relative error ΔS/S of 1% (see figure 5). As before, the errors grows up rapidly as soon as the tetrahedron degenerates to a very flat or a very elongated configuration. If now we increase the heterogeneity factor, for instance h=0.2 (figure 10), the error ΔJ/J grows rapidly, but the conclusion about the shape remains the same.

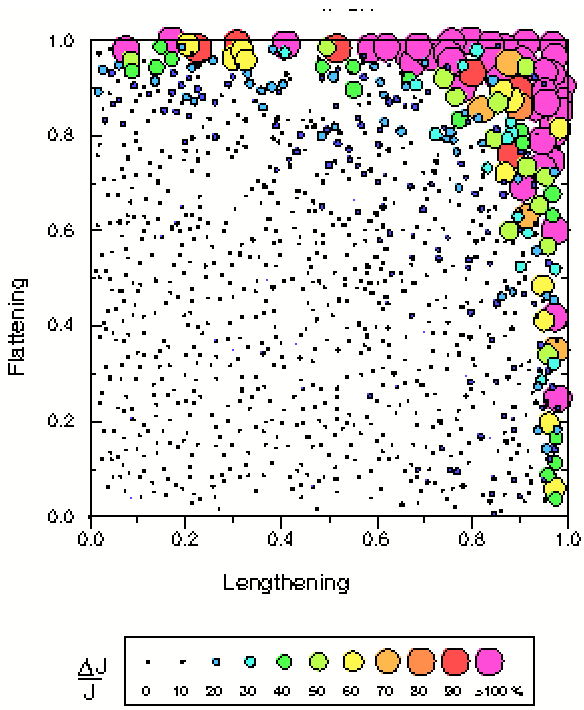

*Figure 9: Influence of the shape of the tetrahedron on the estimate of **J** for a low degree of heterogeneity (h=0.1).*

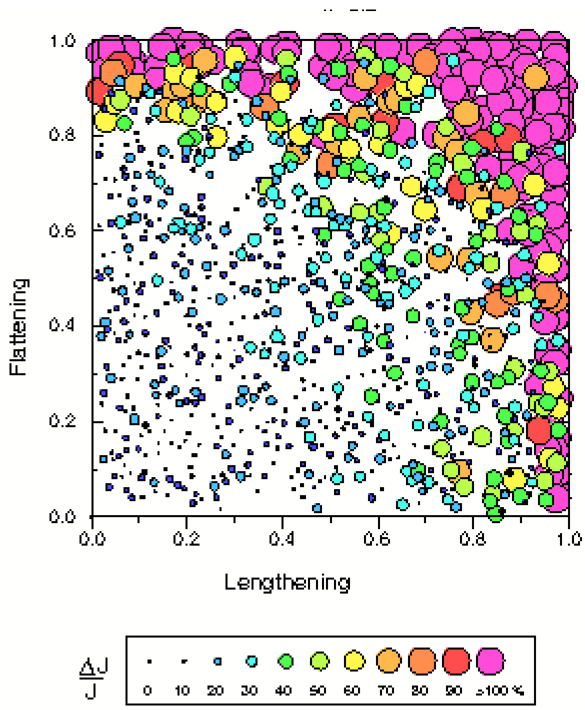

Figure 10: Same as 9, but for a higher degree of heterogeneity (h=0.2).

Nevertheless, it seems that the heterogeneous case is more sensitive to a flat or a linear tetrahedron than the homogeneous case; in other words it seems that the errors due to the linear interpolation are more sensitive for a non regular tetrahedron that the errors associated with uncertainty on ΔS/S or ΔB/B. This is particularly true for the div(**B**)/curl(**B**) ratio: figures 11 and 12 show this ration for h=0.1 and h=0.2, and we can see that the influence of the shape is stronger on this ration than on the accuracy ΔJ/J. Since the errors on div(**B**) and curl(**B**) are unrelated, the total error on the div(**B**)/curl(**B**) ratio is larger.

We have checked that the other conclusions, obtained in homogeneous case, remain the same in heterogeneous case, in particular figure 7 and 8 looks the same with finite value of h. Thus, even in heterogeneous case, there is no correlation between ΔJ/J and div(**B**)/curl(**B**), and the relationship between ΔJ/J and the θ is not obvious, except, maybe, near the limiting values θ=0 or θ=180°.

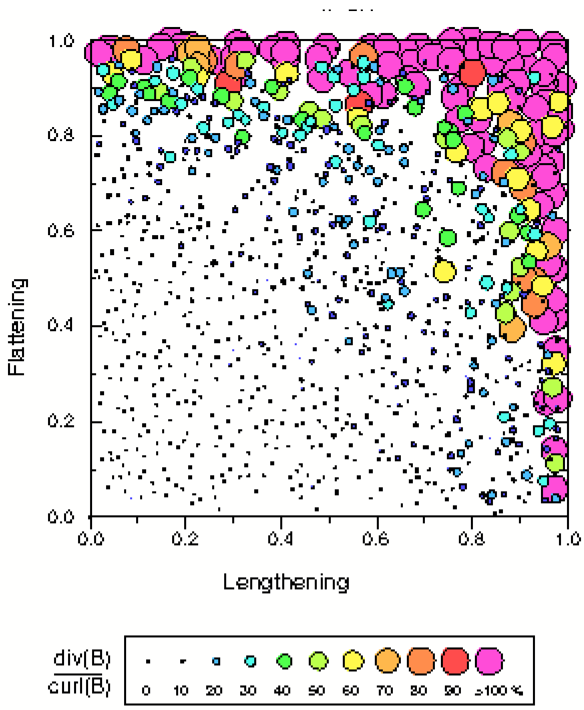

*Figure 11: Influence of the shape of the tetrahedron on the estimated div(**B**)/curl(**B**), for a low degree of heterogeneity (h=0.1).*

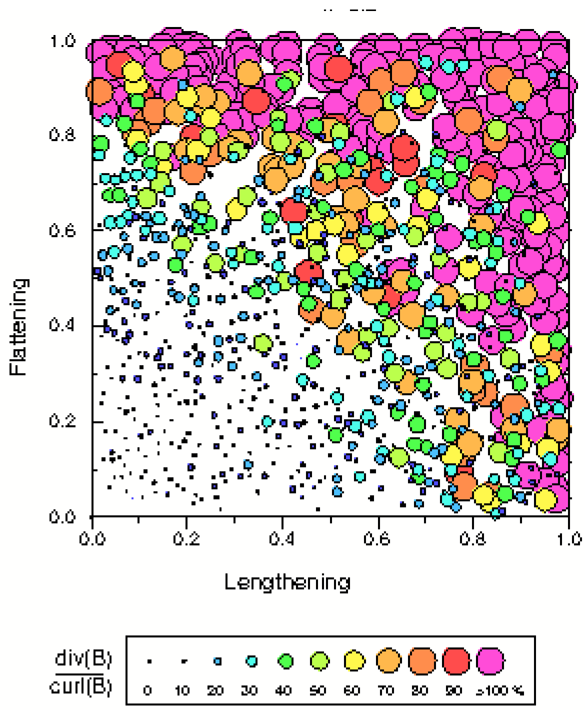

Figure 12: Same as 11, but for a higher degree of heterogeneity (h=0.2).

5. CONCLUSIONS

Characteristic of the shape of the tetrahedron

The inertial ellipsoid is a good approach to characterize the shape of a tetrahedron, and its orientation in space. The L and F parameters allows an appropriate description of this shape with only two quantities, and can be used to defined 5 main types of tetrahedra: "Balls", "Dishes", "Cigars", "Knife Blade" and "Potatoes".
The evolution of the shape of the tetrahedron along Cluster orbit can easily be visualized by displaying it in the L-F diagram, where the shape of the tetrahedron and the accuracy of the determination of the current density can be easily guessed.

Relationship between the shape of the tetrahedron and ΔJ/J

Simulations of the crossing, by 4 S/C, of a current density structure allow an independent estimate of the effects of the various sources of errors, such as the uncertainty on the localisation of the spacecraft, the noise in the magnetometer measurements, and the errors dues to the linear interpolation used for the computation of the various vectorial quantities. These simulations give the relative accuracy ΔJ/J of the measurement versus any significant parameter. In particular the accuracy ΔJ/J has been plotted in a (L,F) diagram, which is very useful to organise the results and to relate easily the shape of the tetrahedron to the accuracy of the estimate of **J** or div(**B**). In particular, the L-F diagram is useful to get a quantitative estimate of this influence, and if, as expected, the regular tetrahedra lead to the most accurate estimates of **J** or div(**B**), the L-F diagram identify a step beyond which the estimate of **J** or div(**B**) is no more valuable. The conclusions are roughly the same for homogeneous case and for heterogeneous case, but it seems that the error due to the linear interpolation in the heterogeneous case is more sensitive to a non regular tetrahedron that the errors due to a relative uncertainty $\Delta S/S$ on the positions. This is particularly true for the div(**B**)/curl(**B**) ratio. In a future work, it would be interesting to try to quantify more precisely the amplitude of the linearization errors versus the heterogeneity parameter.

Relationship between div(**B**)/curl(**B**) and $\Delta J/J$

A potential relationship between div(**B**) and ΔJ has been studied in detail. Statistically, the ratio div(**B**)/curl(**B**) has the same behaviour as $\Delta J/J$. But there is no one to one correspondence. The reason is obvious: since div(**B**) and curl(**B**) are computed from different terms from $\nabla \mathbf{B}$, unless the errors are independent, there is no correlation between div(**B**)/curl(**B**) and $\Delta J/J$. So, during the Cluster mission, if the sources of errors are independent, div(**B**) should not be used as an estimate of the accuracy of the measurement of **J**.

Influence of the direction of the current with respect to the tetrahedron

For a nearly flat tetrahedron, one would expect a strong relationship between the angle θ between the direction of the current and the normal to the main plane of the tetrahedron. This relationship does exist, but only for values of θ very close to 0° or to 180°. Thus, the orientation of the Cluster tetrahedron is not a strong constraint for the estimate of the current density.

REFERENCES

[1] Balogh, A., S.W.H. Cowley, M.W. Dunlop, D.J. Southwood, J.G. Thomlinson, K.H. Glassmeier, G. Musmann, H. Luhr, M.H. Acuna, D.H. Fairfield, J.A. Slavin, W. Riedler, K. Schwingenschuh, F.M. Neubauer, M.G. Kivelson, R.C. Elphic, F. Primdahl, A. Roux, B.T. Tsurutani, The Cluster magnetic field investigation: scientific objectives and instrumentation, 'Cluster: mission, payload and supporting activities', ESA SP-1159, pp 95-114, March 1993.

[2] Robert, P., and A. Roux, Accuracy of the estimate of J via multipoint measurements, in Proceedings of the International Workshop on 'Space Plasma Physics Investigations by CLUSTER and REGATTA', ESA SP-306, pp. 29-35, 1990, (Graz, Autriche, 20-22 février, 1990).

[3] Chanteur, G., Geometrical tools for Cluster data analysis, ESA WPP-047, Proceedings of the International Conference on Spatio-Temporal Analysis for Resolving Plasma Turbulence (START), Aussois, Jan. 31-Febr. 5, 1993, pp. 341-344, 1993.

[4] Robert, P., and A. Roux, Influence of the shape of the tetrahedron on the accuracy of the estimate of the current density, in Proceedings of the ESA Conference on 'Spatio-Temporal Analysis for Resolving plasma Turbulence' [S T A R T], 'Methods for Analysing Plasma Turbulence', ESA WPP 047, pp. 289-294, juin 1993, (Aussois, France, 31 janvier - 05 février, 1993).

[5] Coeur-Joly, O., P. Robert, G. Chanteur, and A. Roux, Simulated daily summaries of Cluster four-point magnetic field measurements, in Proceedings of the ESA Cluster Workshop on ‘Physical Measurements and Mission-Oriented Theory’, ESA SP-371, pp. 223-227, June 1995, (Toulouse, France, 16 17 novembre, 1994).

[6] Robert, P., A. Roux, and O. Coeur-Joly, Validity of the estimate of the current density along Cluster orbit with simulated magnetic data, in Proceedings of the ESA Cluster Workshop on ‘Physical Measurements and Mission-Oriented Theory’, ESA SP-371, pp. 229-233, June 1995, (Toulouse, France, 16 17 novembre, 1994).

[7] Vom Stein, R. , K.-H. Glassmeier, M. Dunlop, A configurational parameter for the Cluster Satellites, Technical Report 2/1992, Institut für Geophysik und Meteorologie, Braunschweig.

[8] Schoenmaekers J., Assessment of Cluster constellation geometry, ESA/ESOC/ECD/OAD, private communication.

[9] Schoenmaekers J., Cluster orbit files, ESA/ESOC/ECD/OAD, private communication.